Atmos. Chem. Phys., 8, 5423–5433, 2008
www.atmos-chem-phys.net/8/5423/2008/

Atmospheric Chemistry and Physics

Inhibition of ice crystallisation in highly viscous aqueous organic acid droplets

B. J. Murray

School of Chemistry, Woodhouse Lane, University of Leeds, Leeds LS2 9JT, UK

Received: 28 March 2008 – Published in Atmos. Chem. Phys. Discuss.: 14 May 2008
Revised: 12 August 2008 – Accepted: 12 August 2008 – Published: 10 September 2008

Abstract. Homogeneous nucleation of ice within aqueous solution droplets and their subsequent crystallisation is thought to play a significant role in upper tropospheric ice cloud formation. It is normally assumed that homogeneous nucleation will take place at a threshold supersaturation, irrespective of the identity of the solute, and that rapid growth of ice particles will follow immediately after nucleation. However, it is shown here through laboratory experiments that droplets may not readily freeze in the very cold tropical tropopause layer (TTL, typical temperatures of 186–200 K). In these experiments ice crystal growth in citric acid solution droplets did not occur when ice nucleated below 197±6 K. Citric acid, 2-hydroxypropane-1,2,3-tricarboxyllic acid, is a molecule with similar functionality to oxygenated organic compounds which are ubiquitous in atmospheric aerosol. It is therefore thought to be a sensible proxy for atmospheric organic material. Evidence is presented that suggests citric acid solution droplets become ultra-viscous and form glassy solids under atmospherically relevant conditions. Diffusion of liquid water molecules to ice nuclei is expected to be very slow in ultra-viscous solution droplets and nucleation is negligible in glassy droplets; this most likely provides an explanation for the experimentally observed inhibition of ice crystallisation. The implications of ultra-viscous and glassy solution droplets for ice cloud formation and supersaturations in the TTL are discussed.

Correspondence to: B. J. Murray
(b.j.murray@Leeds.ac.uk)

1 Introduction

Ice clouds that form in the Earth's upper troposphere (UT) are known to play a significant role in the planet's radiation budget and climate (Liou, 1986), but mankind's impact on these clouds is uncertain (Denman et al., 2007). Ice clouds in the UT also influence the entry of water vapour into the stratosphere by acting as a cold trap (Jensen and Pfister, 2005), and they provide a surface on which chemical species may adsorb and react (Abbatt, 2003). A quantitative knowledge of the fundamental ice nucleation and crystallisation processes of these clouds is essential in order to understand and predict their impact on the Earth's atmosphere and climate.

An important mechanism of UT ice cloud formation is through the homogeneous freezing of aqueous solution droplets. Homogeneous freezing is a multi-step process; it begins with nucleation of ice which then triggers ice crystal growth and the resulting aqueous brine may also crystallise to form a crystalline solute phase or phases (Murray and Bertram, 2008). Ice crystal growth may then continue by deposition from the vapour phase until the water vapour supersaturation is relaxed and ice particles exist in equilibrium with the surrounding atmosphere. In a landmark paper Koop et al. (2000) showed that homogeneous nucleation in aqueous solution droplets only depends on water activity (a_w) for a wide range of solution droplets. The water activity of droplets at equilibrium equals the relative humidity (with respect to liquid water, RH_w) of the surrounding atmosphere (i.e. a_w=RH_w/100, at equilibrium). Hence the homogeneous freezing threshold can be defined in terms of RH_w; this greatly simplified the description of homogeneous freezing in cloud formation models. However, recent observations of very high supersaturations both in and out of very cold ice clouds in the tropical tropopause layer (TTL, ∼11–18 km, typically ∼185–200 K, Gettelman and Forster, 2002) have brought into question our fundamental understanding of

Published by Copernicus Publications on behalf of the European Geosciences Union.

cold ice cloud formation (Jensen and Pfister, 2005; Peter et al., 2006; Jensen et al., 2005; Gao et al., 2004).

In general, ice nucleation in aqueous inorganic systems, which have been tested to low temperature (<200 K) is consistent with the water activity criterion (Koop, 2004; Murray and Bertram, 2008). However, very few studies exist in which homogeneous freezing has been measured in aqueous organic solution droplets (Prenni et al., 2001; Wise et al., 2004; Zobrist et al., 2006) and none have been performed for conditions relevant to the TTL (i.e. <200 K).

Organic material accounts for up to 70% of the mass of fine aerosol in the troposphere (McFiggans et al., 2005). Much of this organic material is oxygenated and COOH, OH and C=O functional groups are ubiquitous (Graber and Rudich, 2006; Saxena and Hildemann, 1996). In-situ single particle mass spectrometry measurements of UT aerosol confirm that oxygenated organic material is usually present, and in some cases organic material is the dominant component of aerosol (Cziczo et al., 2004a, b; Murphy et al., 2006, 1998; Zobrist et al., 2006). An important property of oxygenated organic compounds is their ability to form extensive hydrogen bonding; therefore molecules of relatively large mass may be soluble in water.

It is well known in the food industry and the field of biological tissue preservation that the addition of oxygenated organic compounds, such as sugars, to aqueous solution can lead to the formation of glassy solids (Angell, 2002). These glassy solids form at temperatures which are relevant to the Earth's atmosphere. A glassy solid is a solid in which the arrangement of its constituent molecules lacks long range order, i.e. they are amorphous rather than crystalline. Glassy solids form if a liquid is cooled to a sufficiently low temperature so that the molecules effectively cease to diffuse and become locked in a "liquid-like" amorphous state. The threshold temperature where an ultra-viscous liquid becomes glassy is known as the glass transition temperature (T_g). The viscosity of a substance at glass transition is on the order of 10^{14} cP, some 14 orders of magnitude larger than that of water at room temperature. The impact of highly viscous and glassy solution droplets on the Earth's atmosphere and cloud formation is at present unknown.

There is mounting evidence that organic-rich aerosol in the atmosphere behave differently to sulphate aerosol. Cziczo et al. (2004a) found organic-rich particles preferentially remain unfrozen. DeMott et al. (2003) used a thermal diffusion chamber at 229 K and a single particle mass spectrometer to show that aerosols composed of organics froze at a significantly higher saturation threshold than sulphate aerosol. In a set of expansion chamber experiments Möhler et al. (2005) found that soot composed of 40% organic carbon nucleated ice inefficiently even at an RH_{Ih} (relative humidity with respect to hexagonal ice) of 190%; this is well above the nucleation threshold defined by the water activity criterion (RH_{Ih}~160%).

In the present experimental study, the crystallisation of aqueous citric acid (2-hydroxypropane-1,2,3-tricarboxyllic acid, $C_6H_8O_7$) solution droplets have been investigated using X-ray diffraction. Citric acid was chosen for this study for two main reasons. First, it contains one hydroxyl (OH) and three carboxylic (COOH) functional groups and therefore has similar functionality to many compounds in atmospheric aerosol. Indeed, it has been observed as a minor component of atmospheric aerosol (Saxena and Hildemann, 1996; Falkovich et al., 2005). The second reason for choosing citric acid for these experiments is that the physical properties of aqueous citric acid solutions have already been characterised since it is a common ingredient in food and pharmaceutical products. The properties include the glass transition temperature (Maltini et al., 1997).

The objective of this laboratory investigation was to investigate the impact of an oxygenated organic compound relevant to the Earth's atmosphere on the nucleation and growth of ice crystals in aqueous droplets. In order to do this, droplets of known composition were frozen within an X-ray diffractometer. The resulting diffraction patterns of the droplets were used to determine the phase change temperatures and also the quantity of ice that crystallised. It was found that the crystallisation of ice is incomplete below ~197 K. It is shown that this inhibition of crystallisation is most likely to be related to the high viscosity and glass formation in citric acid solutions at temperatures relevant for the TTL. Finally, the implications of highly viscous or glassy solution droplets for UT cloud formation are discussed.

2 Experimental

The experimental technique was recently described in detail (Murray, 2008) and will only be summarised here. In order to investigate the crystallisation process and inhibition of ice crystallisation in solution droplets, a powder X-ray diffractometer equipped with a cold stage was employed. Aqueous solution droplets of between 0 and 61.2 wt% (volume median diameter between 5–10 μm) were suspended in an oil matrix containing lanolin. These emulsions were placed on a cold stage within the diffractometer. The temperature of these emulsified aqueous droplets could then be altered in a controlled way, therefore the temperatures of phase changes and also the phases that formed were determined. Samples were cooled at an average rate of 5 ± 1 K min^{-1} to 173 K, while monitoring the 2θ=40° Bragg peak for ice crystallisation; thus freezing temperatures were determinded. At low temperature (173 K) the full diffraction pattern was measured between 2θ=20 and 50°, which covers all major peaks in both cubic and hexagonal ice. Ice crystallisation was also measured on warming by increasing temperature at an average ramp of 5 ± 1 K min^{-1}. Ice crystallisation on warming is referred to as warm ice crystallisation. An average ramp of

$1\pm0.1\,\mathrm{K\,min^{-1}}$ was used to determine ice melting temperatures.

A number of advantages of employing emulsified samples were listed by Murray (2008); one advantage is that there is no significant preferred crystallographic orientation when ice crystallises in emulsified samples. Orientation of crystals results in changes in the relative intensities of the diffraction peaks and can complicate interpretation of the resulting diffraction data. Rietveld refinements of frozen emulsified solution droplets (which crystallised to hexagonal ice, letovicite and sulphuric acid tetrahydrate) conclusively demonstrate that the crystallographic orientation of each frozen droplet is random and that there is no overall preferred orientation (Murray and Bertram, 2008).

The rate of transfer of heat evolved during crystallisation to a droplet's surroundings should be considered when interpreting data from emulsified samples. Heat transfer calculations (see Murray and Bertram, 2006; Murray et al., 2005) show that when crystal growth and resulting latent heat release is rapid, such as in pure water, droplets will heat up more when suspended in gas than if in an oil matrix. However, ice crystallisation and corresponding heat release in micrometer sized concentrated solution droplets (in which ice I_c forms) is slow relative to heat dissipation in either oil or gas and these droplets do not heat up significantly. Hence, the results presented here for concentrated solution droplets, where crystallisation is relatively slow, are directly relevant to the atmosphere.

3 Results and discussion

3.1 Diffraction patterns of frozen droplets

Examples of typical diffraction patterns of citric acid solution droplets which had been cooled to 173 K at $5\,\mathrm{K\,min^{-1}}$ are shown in Fig. 1. There are clearly some very strong differences between these patterns. Pattern 1a is of frozen 10.8 wt% solution droplets which froze at 229±6 K. This pattern is consistent with previous diffraction patterns of a mixture of cubic ice (ice I_c) and hexagonal ice (ice I_h) (Murray and Bertram, 2006, 2007a, b; Murray et al., 2005). Patterns 1b and c are of more concentrated solution droplets which froze at 209±6 and 199±6 K, respectively. In these patterns several of the peaks unique to hexagonal ice are absent and the patterns are consistent with ice I_c with stacking faults (Murray et al., 2005). The hexagonal peak at ∼23° remains in these cubic ice patterns, whereas it is clear from the absence of other hexagonal peaks that no bulk hexagonal ice crystallised. This feature is thought to be related to stacking faults in the cubic structure (Murray et al., 2005). All of the peaks can be attributed to ice and it is concluded that no citric acid phases crystallised. Stacking faults are also known to cause some broadening of Bragg peaks and also asymmetry in Bragg peaks. In the absence of a method to quantify the impact of stacking faults, an analysis of the size of ice crystallites based on peak widths has not been attempted.

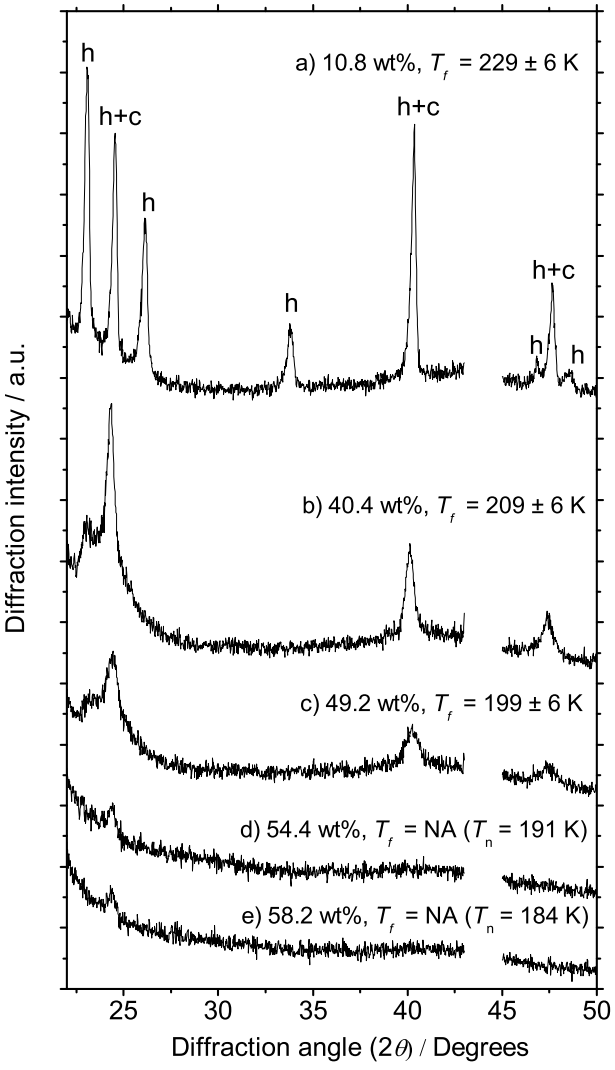

Fig. 1. Examples of diffraction patterns of citric acid solution droplets recorded at 173 K. Regions of the diffraction patterns influenced by the cell construction materials have been removed. The predicted ice nucleation temperatures (T_n) were determined using the method outlined in Sect. 3.2.

A strong solute dependence of the ice phase has been observed in the past, with $(NH_4)_3H(SO_4)_2$ freezing to ice I_c below 200 K, whereas a similar amount of ice I_c will only form below 183 K in NH_4HSO_4 solution droplets (Murray and Bertram, 2007b; Murray and Bertram, 2008). It seems that citric acid solution droplets have an even greater propensity to freeze to the metastable ice Ic than $(NH_4)_3H(SO_4)_2$ droplets, with a threshold ∼20 K higher. The issue of ice phase in organic solution droplets has been addressed in a separate manuscript (Murray, 2008) and will not be discussed further here.

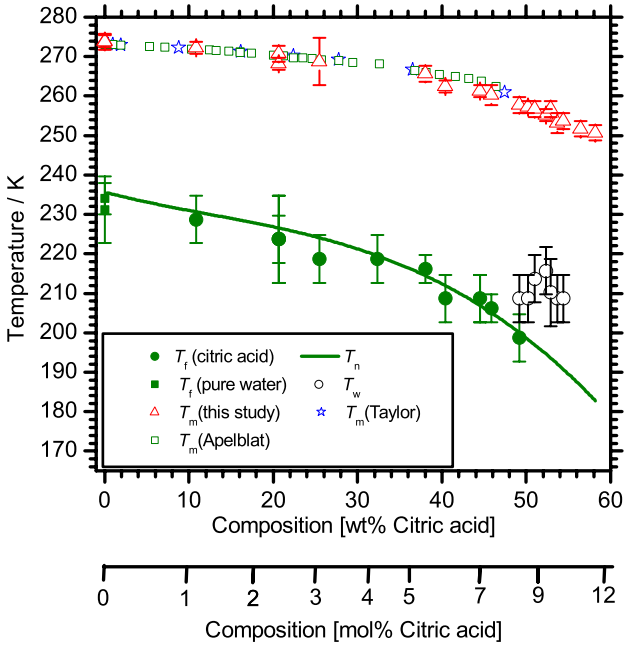

Fig. 2. State diagram for the citric acid-water system. The measured ice melting temperatures (red open triangles) and the freezing temperatures (filled green circles) are reproduced from Murray (2008). The melting temperatures are compared with literature values; green open squares (Apelblat, 2003) and blue stars (Taylor, 1926). The temperatures at which ice crystallisation was observed on warming are plotted as black open circles. The solid green line is the predicted ice nucleation temperature based on the relationship between the freezing and measured melting point depressions; see Fig. 3 and the text for details.

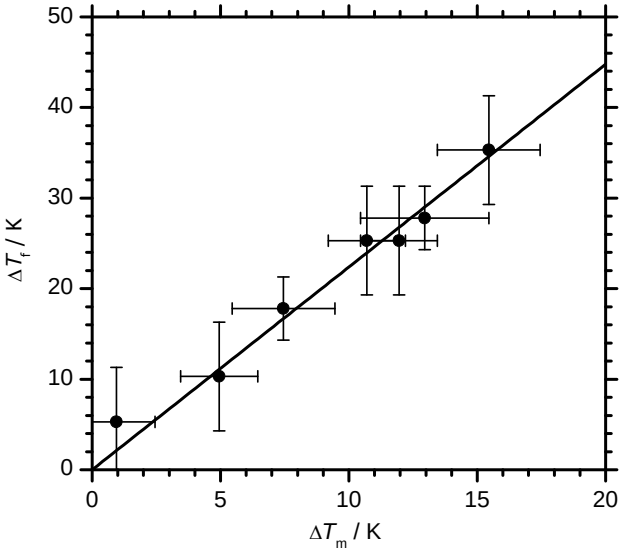

Fig. 3. The freezing temperature depression as a function of the melting point depression. See text for details. The solid line is a best fit forced through the origin (slope=λ=2.24±0.06).

The patterns shown in Fig. 1d and e are that of droplets of 54.4 and 58.2 wt% citric acid, respectively, which were cooled to 173 K at the standard rate of 5 K min^{-1}. The major ice peaks at 2θ=40 and 47° (common to both ice I_c and ice I_h) are absent, indicating that no bulk ice crystallised. There is a hint of an ice peak at 2θ=24°, which indicates that there is limited crystalline nature and that ice nucleation may have begun, but did not continue. The inhibition of crystallisation will be discussed at length later in this paper.

3.2 Phase changes in the citric acid-water system

The temperatures at which freezing (T_f), ice crystallisation on warming (T_w) and ice melting (T_m) occurred are plotted in Fig. 2. This diagram is referred to as a state diagram, rather than a phase diagram, since both equilibrium and kinetically controlled phase changes are shown. Previous measurements of T_m of citric acid solutions are also plotted and are in agreement with those from the present study. In addition, the melting and freezing temperatures of pure water are consistent with literature values.

Freezing temperatures have been recorded for droplets with concentrations up to 49.2 wt%. Insufficient ice crystallised in droplets of higher concentration to identify a freezing temperature (the technique for measuring crystallisation temperatures with XRD is sensitive to ∼10 wt% of the overall mass of the droplets changing phase). Ice crystallisation was not observed in droplets of >49.2 wt% on cooling, but in some cases ice crystal growth was detected at (T_w=)211±6 K as the droplets were warmed at 5 K min^{-1}. T_w was measured between 49.2 and 54.4 wt%. For concentrations between 54.4 and 58.2 wt% T_w was not determined, however, ice did crystallise on warming at some temperature below the ice-liquid equilibrium curve and T_m could then be determined. The fact that ice crystallised on warming droplets of between 49.2 and 58.2 wt% indicates that nucleation of ice took place at some lower temperature, but crystal growth rates only became comparable to the warming rate at around 211 K or above. X-ray diffraction is insensitive to nanometer-sized crystals, and therefore insensitive to critical clusters, hence the lack of Bragg diffraction peaks only indicates that bulk ice crystals did not form. These droplets formed what is referred to as X-ray amorphous materials, i.e. material lacking bulk ice crystals which have diffraction patterns that lack distinct Bragg diffraction peaks, but in which nanocrystalline ice may exist. This nanocrystalline ice then provided the seed from which larger ice crystals grew at higher temperatures.

Droplets with concentrations of 59.6 and 61.2 wt% did not crystallise on cooling to 173 K or on subsequent warming, indicating that nucleation of ice did not occur in these very concentrated solution droplets. These droplets most likely formed true glassy solids (i.e. an amorphous solid with the

absence of any crystalline or nanocrystalline ice) before they became sufficiently supersaturated for nucleation, hence nucleation was inhibited and they therefore did not crystallise on cooling or warming. This will be discussed in more detail in Sects. 3.3 and 3.4.

It has been shown in the past that the homogeneous freezing temperature depression of an aqueous solution $\Delta T_f = T_f$ (Pure H_2O) $- T_f$ (solution) increases in direct proportion to the melting point depression $\Delta T_m = T_m$ (Pure H_2O) $- T_m$ (solution). This is true for a wide range of inorganic (DeMott, 2002) and organic solutions (Zobrist et al., 2003). Figure 3 shows that citric acid solution droplets behave in a similar manner, with a slope, λ ($\Delta T_f / \Delta T_m$), of 2.24±0.06. Literature values for smaller solute molecules (e.g. H_2SO_4, NaCl, KCl, etc.) have λ values of between 1.4–2.2, while larger more complex molecules capable of extensive hydrogen bonding have λ values up to 5.1 (Zobrist et al., 2003). Zobrist et al. (2003) suggest that the more extensive hydrogen bonding between oxygenated organic molecules and water, compared to many inorganic solutes, leads to larger values of λ.

If it is assumed that the delay between nucleation and crystallisation is negligible for the points shown in Fig. 3, it can be said that the measured ΔT_f is the same as the nucleation point depression (ΔT_n). Hence, the relationship $\Delta T_n = \lambda \Delta T_m$ (λ=2.24±0.06) can be used to estimate T_n in the cases where freezing was not observed, but where ice crystallised on warming and T_m was measured. In Fig. 2, values of T_n based on this relationship have been plotted for citric acid concentrations from 0 to 58.2 wt%, where T_m was measured experimentally.

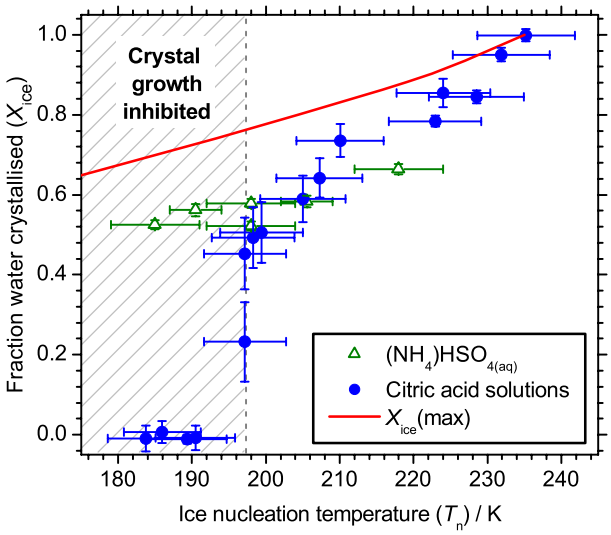

Fig. 4. The fraction of water in solution droplets which crystallised to ice (X_{ice}) when cooled to 173 K at a rate of 5 K min^{-1}, expressed as a function of ice nucleation temperature. Data for citric acid is plotted as blue filled circles. An X_{ice} value of 1 indicates all water crystallised and a value of 0 indicates none crystallised. The nucleation temperature was determined using the relationship between the ice freezing and ice melting point depression (i.e. $\Delta T_n = \lambda \Delta T_m$, where λ2.24±0.06, see text for details). The solid red line is the maximum X_{ice} in citric acid solution droplets; i.e. it is the X_{ice} for ice in equilibrium with an aqueous citric acid brine at 173 K assuming there are no kinetic limitations to ice crystallisation and the citric acid does not crystallise to a solid citric acid phase. X_{ice} is also plotted for ammonium bisulphate solution droplets using an identical experimental procedure (green open triangles).

3.3 Inhibition of ice crystallisation

In Fig. 4, the fraction of water which crystallised to ice ($X_{ice} = M_{ice}/(M_{ice}+M_{liq})$, where M_{ice} is the mass of ice and M_{liq} is the mass of water in the aqueous phase, is plotted as a function of ice nucleation temperature (T_n). X_{ice} was determined by measuring the area under the ice peak at 2θ=40° in the full diffraction patterns recorded at 173 K (such as those in Fig. 1). Peak areas were determined by fitting a Gaussian profile to the pertinent peak using a least-squared routine and integrating the area under the fitted profile. This technique was used in the past to deconvolute overlapping peaks (Murray and Bertram, 2007b). The area of this peak, I_{40}, was then normalised to the weight fraction of water in the solution droplets, W_{H_2O}, and the weight fraction of solution in the oil phase, W_{sol}, i.e. the normalised peak area, $L_{40} = I_{40}/W_{H_2O}/W_{sol}$. The normalized peak area of the frozen solution droplets was then divided by the value for frozen pure water droplets in order to obtain the fraction of water crystallised, i.e. $X_{ice} = L40(\text{solution})/L_{40}$ (pure H_2O) and since diffraction intensity is proportional to mass $X_{ice} = M_{ice}/(M_{ice}+M_{liq})$. It is assumed here that 100% of water in pure water droplets crystallises to ice. Hence, a value of 1 indicates 100% of the water crystallised and 0 indicates 0% of the water crystallised.

The maximum fraction of water that can crystallise (X_{ice} (max)) in aqueous citric acid solution droplets, assuming there are no kinetic limitations to ice crystal growth and that the solute phase does not crystallise, is shown in Fig. 4. When ice crystallises in a solution droplet it will exist in equilibrium with aqueous brine if there are no kinetic limitations to crystal growth. Hence some fraction of water will necessarily be in the aqueous phase and X_{ice} (max) will therefore be less than unity when ice forms in a solution. In the experiments presented here, citric acid was not observed to crystallise, hence when ice formed it was always internally mixed with aqueous citric acid solution. If ice was in equilibrium with aqueous citric acid when the full diffraction patterns were measured at 173 K, then the concentration of this solution would dictate X_{ice} (max) for a particular initial solution concentration. The determination of the ice-liquid line in Fig. 3 is described in Appendix A, and it was found that the concentration of an aqueous citric acid brine in equilibrium with ice at 173 K was 83.0 wt%. The increase in aqueous phase concentration from the initial solution before ice

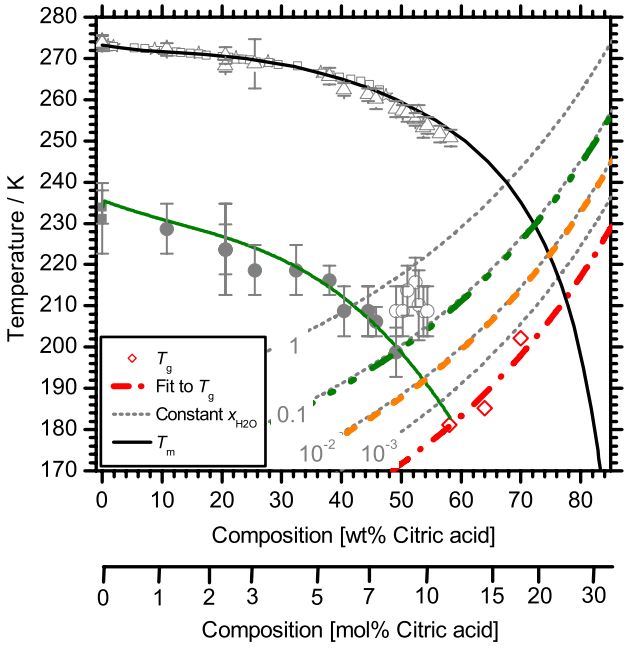

Fig. 5. State diagram including glass transition temperatures and mean diffusion distances for the citric acid-water system. The black solid line is an estimate of the ice-liquid equilibrium line based on water activity data; see Appendix A for details. The experimental data for melting, freezing and ice crystal growth on warming from Fig. 2 have been included for comparison as grey symbols. The predicted T_n line from Fig. 2 is also included as a solid green line. Literature data for the glass transition temperature measured by differential scanning calorimetry together with a parameterisation for this data are shown as red open diamonds and a dot-dashed line, respectively. The dotted grey lines are lines of constant mean diffusion distance (x_{H_2O}) of water molecules and are taken from Murray (2008) (see Appendix B for a summary of how these lines were determined). The labels indicate the root mean square distance (micrometers) water molecules are expected to diffuse in 1 min. The dot-dot-dashed green line represents the approximate limiting value of x_{H_2O} (0.09 μm) below which ice crystal growth is inhibited at a cooling rate of 5 K min^{-1}, whereas the dashed orange line represents the x_{H_2O} (0.009 μm) below which ice crystal growth is estimated to be inhibited at a cooling rate of 0.5 K min^{-1}.

formation to the final concentration after ice formation is due to water being removed from the aqueous phase to form ice; hence the X_{ice} (max) was quantified.

Inspection of Fig. 4 reveals that the experimentally determined values of X_{ice} are significantly smaller than X_{ice} (max), in all cases except for very dilute solution or pure water. This indicates that there is some kinetic limitation to ice crystal growth. In fact, X_{ice} drops dramatically below 197±6 K, indicating that crystallisation of ice is strongly inhibited below this temperature when cooled at 5 K min^{-1}. No detectable bulk ice crystallised in these droplets (i.e. less than 3% of the available water crystallised, as determined from the full diffraction patterns which were collected over 30–40 min at 173 K). This is an important finding since it is generally assumed that ice will nucleate and grow in aqueous droplets under conditions relevant for the Earth's troposphere. In fact, ice crystallised readily in NH_4HSO_4 solution droplets at temperatures well below 197 K (open green triangles in Fig. 4), in agreement with previous experiments (Koop et al., 1999; Murray and Bertram, 2008). The freezing of citric acid solution droplets clearly contrasts with that of NH_4HSO_4 droplets and may have important implications for ice cloud formation in the TTL region. These implications are discussed later in this paper.

3.4 The formation of highly viscous or glassy solution droplets

The experiments presented here show that ice crystallisation is inhibited in citric acid solution droplets at ice nucleation temperatures below 197±6 K. It is suggested here that these solution droplets become highly viscous or even glassy and crystallisation is therefore inhibited. Unfortunately, no direct measurements exist of diffusion in low temperature citric acid solution droplets. However, the glass transition temperature (T_g) for several pertinent concentrations of citric acid solution have been measured and fitted (Maltini et al., 1997); these are plotted in Fig. 5. The T_g provides a useful reference temperature from which viscosity and diffusion can be estimated at higher temperatures. The measured and fitted T_g's have been used to estimate the root mean square distance water molecules diffuse in 60 s (x_{H_2O}) and lines of constant x_{H_2O} are plotted in Fig. 5. The derivation of x_{H_2O} is described in Appendix B.

The lines of constant x_{H_2O} in Fig. 5 (values are in micrometers) provide a useful means by which to gauge if a droplet is likely to crystallise. The exact relationship between diffusion and crystal growth is complicated. However, it is true that if x_{H_2O} is much smaller than the dimensions of the droplets then ice will not readily crystallise.

Inspection of Fig. 5 shows that in general, molecular diffusion decreases dramatically as concentration increases and temperature decreases. It is clear from Fig. 4 that the crystallisation did not occur below 197±6 K in droplets which were cooled to 173 K at a rate of 5 K min^{-1}. This corresponds to a diffusion distance of 0.09 μm in Fig. 5 and defines x_{H_2O} below which crystallisation at a cooling rate of 5 K min^{-1} is limited by diffusion. Crystallisation only occurs on warming these solution droplets (at 5 K min^{-1}) when x_{H_2O}>0.09 μm. The x_{H_2O} contour for x_{H_2O}=0.09 μm is plotted as a green dot-dot-dashed line in Fig. 5 and represents the limiting condition for crystal growth for a warming or cooling rate of 5 K min^{-1}. At temperatures above this line, crystal growth is rapid on the minute timescale, whereas at lower temperatures ice crystal growth is slow.

Droplets were cooled at a rate of 5 K min^{-1} in these experiments, which is significantly faster than typical cooling rates

leading to cirrus cloud formation (0.0007 to 0.7 K min^{-1}, Jensen et al., 2005). The threshold of 197 K, below which ice crystallisation becomes inhibited at a cooling rate of 5 K min^{-1}, will shift to lower temperatures for slower cooling rates. If an air parcel is cooling at 0.5 K min^{-1}, then the time available for crystal growth will be a factor of ten greater than in the experiments with cooling at 5 K min^{-1}. Hence, it can be stated that crystallisation will only become inhibited when $x_{H_2O} > 0.009\,\mu$m (the orange line in Fig. 5) and that this corresponds to a T_n of 192 K.

In droplets of 59.6 and 61.2 wt% no crystallisation was observed on cooling to 173 K, leaving them at 173 K for ∼40 minutes or on warming them at 5 K min^{-1}. It appears that the nucleation of ice itself was inhibited. Inspection of the predicted nucleation temperature of ice in citric acid droplets in Fig. 5 reveals that the nucleation temperature intercepts T_g at around 58.5 wt% and 180 K. This is consistent with the measurement showing that nucleation does not take place in 59.6 and 61.2 wt% solution droplets; in fact, these droplets most likely formed glassy solids. Hence, the point where the homogeneous freezing temperature and glass transition temperature intercept represents a limit of nucleation. At higher concentrations than 58.5 wt%, the solution only becomes sufficiently supersaturated for homogeneous nucleation at temperatures below the glass transition, hence nucleation of ice did not occur.

In an investigation of freezing in aqueous H_2SO_4 solution droplets Koop et al. (1998) found that droplets of concentration greater than 26.7 wt% did not crystallise on cooling, but did on warming at 10 K min^{-1} between 165 and 172 K. Bogdan et al. (2006) made a similar observation in 31.5 wt% H_2SO_4 solution droplets, although the crystallisation on warming at 3 K min^{-1} took place at ∼156 K. This behaviour is similar to citric acid solutions, except that crystallisation occurred at much lower temperatures in aqueous H_2SO_4. This indicates that diffusion becomes rapid, in comparison to ramp rate, at much lower temperatures in H_2SO_4 solutions than in citric acid solutions. In fact, the glass transition measured by Bogdan (for 31.5 wt% H_2SO_4 droplets) was at ∼142 K; this is about 14 K below the temperature at which the droplets crystallised when warming at 3 K min^{-1}. Given that crystallisation becomes rapid in H_2SO_4 solutions at temperatures well below those typical for the Earth's troposphere, ice would be expected to form in these aerosols efficiently and in accord with the water activity criterion (Koop et al., 2000). In citric acid solution droplets ice formation may occur at a slower rate or may even be inhibited.

It is well known that T_g of aqueous solutions depends strongly on the solute type. In fact, Zobrist et al. (2008) have very recently demonstrated that T_g for a number of aqueous inorganic solutions are much lower than for a number of atmospherically relevant organic acid and polyol solutions. They conclude that aqueous organic droplets may form glasses in the atmosphere. This is consistent with the results of the present study.

4 Atmospheric implications and summary

The primary conclusion from this experimental study is that ice does not necessarily crystallise in aqueous solution droplets even if they are sufficiently supersaturated for homogeneous nucleation. The growth of ice crystals in citric acid droplets is much slower below 197±6 K than in ammonium bisulphate (or sulphuric acid) solution droplets and does not occur when cooled at 5 K min^{-1}. It is argued that crystallisation is limited by slow diffusion in these highly viscous or glassy solution droplets. It is predicted that ice crystal growth is limited below ∼192 K at an atmospherically relevant cooling rate of 0.5 K min^{-1}. Nucleation does not occur in solution droplets where sufficient supersaturation for nucleation is only attained below the glass transition temperature; in the case of aqueous citric acid this threshold is at ∼180 K. This work extends that of Koop et al. (2000) who showed that the temperature at which ice nucleates homogeneously is a function of water activity only. Here, it is argued that solution viscosity plays a critical role in i) the growth of ice crystals within solution droplets and ii) the nucleation of ice.

The inhibition of ice crystallisation may have important implications for cloud formation in the tropical tropopause layer where temperatures are regularly as low as ∼186 K (Zhou et al., 2004). If the crystallisation of ice is inhibited within atmospheric aqueous solution droplets in an ascending air mass, then the humidity will exceed the limit defined by the water activity criterion (Koop et al., 2000). In fact, field measurements appear to show extreme supersaturations, with RH_{Ih} in excess of 200% with no apparent ice cloud formation (Jensen et al., 2005). These very high supersaturations were observed in air that was below 190 K. This is in the temperature range where organic acids, similar to citric acid, might inhibit ice crystallisation, but where sulphate aerosols would be expected to freeze readily and lead to cloud formation. It is suggested here that very high supersaturations might from in any cold air mass where the aerosol contains sufficient oxygenated organic material to inhibit ice crystallisation. Unfortunately, no composition data were obtained on the aerosol in this layer of very high supersaturation observed by Jensen et al. (2005). However, particles sampled nearby were composed of typical sulphate-organic mixtures (Jensen et al., 2005).

Atmospheric aerosols contain a massive range of organic species (Saxena and Hildemann, 1996) usually internally mixed with sulphate (Murphy et al., 2006), hence real aqueous droplets will have a range of viscosities. The ubiquity of carboxylic, hydroxyl, carbonyl and other functional groups, which are capable of hydrogen bonding, in the organic fraction of aerosol suggests that many oxygenated organic solutes will have a similar impact on freezing to citric acid. It is possible some will slow crystal growth even more dramatically than citric acid, while others will behave more like sulphate aerosol. Further experiments are required to test crystallisation in other aqueous oxygenated organic solutions and

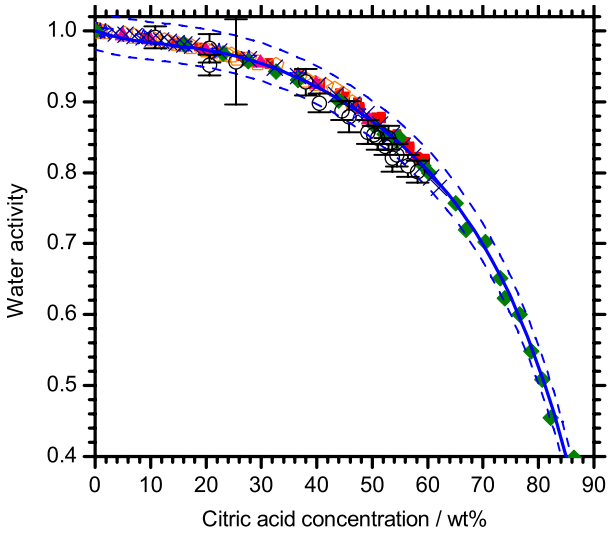

Fig. A1. Water activity data as a function of citric acid concentration. See Table A1 for data sources and a key to the symbols. The solid line is a polynomial fit between 0 and 85 wt%, and the dashed lines represent 95% prediction limits.

also in aqueous organic-sulphate mixtures.

This study represents a first step in understanding the role of viscosity in cold ice cloud formation. While it is clearly shown that ice crystallisation can be inhibited in citric acid solution droplets, it should be noted that the trajectory through the temperature-composition phase diagram is very different in the experiments presented here and for droplets in the atmosphere. In the experiments presented here, solution concentration is fixed by locking droplets in an oil emulsion and droplets are then cooled. However, aerosols in an atmospheric air parcel will take up water to become more dilute as they cool down, only freezing when they become sufficiently dilute and cold. However, in the case of citric acid solution droplets this will involve starting with highly concentrated solution droplets on the right hand side of Fig. 5 which may already be highly viscous or glassy. If droplets start off in a highly viscous or glassy state then it is unlikely that they will take up water and dilute. Hence, the droplets may not become sufficiently dilute for ice to nucleate homogeneously within them.

On account of both the inhibition of ice crystallisation and the likely limited uptake of water into highly viscous organic acid solution droplets, it seems probable that ice crystallisation should be preferred in atmospheric droplets rich in sulphate. In fact, in a single particle mass spectrometry study of cirrus ice crystals and aerosol (mentioned in the introduction) Cziczo et al. (2004a) found that sulphate preferentially partitioned to the ice phase over organic material. In a modelling study, Kärcher and Koop (2005) suggested reduced water uptake into organic aerosol might explain this observation. Reduced water uptake might be caused by a smaller accommodation coefficient or a lower water content at equilibrium relative to inorganic aerosol, resulting in smaller droplets which are less likely to freeze. An alternative explanation for the observation is that organic-containing droplets are highly viscous at sufficiently low temperatures and therefore i) do not take up water as efficiently as aqueous sulphate droplets and ii) even if ice does nucleate, crystal growth rates are slower than in sulphate droplets.

In order to fully assess the impact of ultra-viscous liquids and glassy solids on cloud formation, further research is needed. This should include measurements of ice crystallisation in solution droplets with solutes other than citric acid, water uptake into viscous droplets and cloud chamber simulations in order to follow a more atmospherically relevant temperature-RH trajectory. Nevertheless, in this paper it has been shown that droplets which contain a solute of similar functionality to many molecules ubiquitous in the troposphere appear to become highly viscous or glassy under TTL conditions and crystallisation of ice can be inhibited.

Appendix A

Determination of the hexagonal ice-liquid equilibrium curve

The ice-liquid curve has been described in terms of solution water activity (a_w) between 150 and 273 K and is independent of solute type (see Eqs. 1 and 2 in Koop et al., 2000). In order to plot the ice-liquid equilibrium curve as a function of citric acid solution concentration (as it is in Fig. 5) the relationship between a_w and solution concentration must be known. Values of a_w as a function of citric acid concentration are plotted in Fig. A1 and a list of data sources is given in Table A1. Some of the sources of data quote values of a_w which are plotted in Fig. A1 unaltered (Levien, 1955; Maffia and Meirelles, 2001; Peng et al., 2001). Apelblat et al. (1995) quote the difference in vapour pressure between pure water and an aqueous citric acid solution. These data were used to derive a_w using the known vapour pressure of pure water (Murphy and Koop, 2005). As mentioned above, there is a direct relationship between a_w and ice melting temperatures. Hence, melting temperatures can be used as a measure of a_w. Using Eqs. (1) and (2) from Koop et al. (2000), water activity was determined from ice melting temperatures from the literature (Apelblat, 2003; Taylor, 1926) and from the current experiments.

The data in Fig. A1 between 0 and 85 wt% have been parameterised using a polynomial equation of the form

$$a_w = A + Bc + Cc^2 + Dc^3 + Ec^4 + Fc^5 \quad \text{(A1)}$$

where c is the concentration in wt% and A=1, B=-2.3900×10^{-3}, C=1.5000×10^{-4}, D=-6.1599×10^{-6}, E=8.7490×10^{-8} and F=-5.1132×10^{-10}. Uncertainty in the higher concentration data (>85 wt%) increases, possibly

Table A1. Literature data used to determine the relationship between a_w and citric acid solution concentration.

Temperature range/K	Concentration range/wt%	Reported quantity	Reference	Points in Fig. A1
298.13–319.33	8.94–59.51	p_{H_2O}	(Apelblat et al., 1995)	Red filled squares
298.15	4.99–49.48	a_w	(Maffia and Meirelles, 2001)	Pink filled triangles
289.15	0.00–93.89	a_w	(Peng et al., 2001)	Green filled diamonds
298	3.7–61.99	a_w	(Levien, 1955)	Blue crosses (X)
260.9–273.1	0.19–47.45	T_m	(Taylor, 1926)	Blue hollow stars
273.14–262.45	0.013–46.4	T_m	(Apelblat, 2003)	Orange hollow pentagons
250.7–272.2	10.83–58.21	T_m	This study	Black hollow circles

due to the very high viscosity of extremely concentrated citric acid solution, and this data was therefore not included in this fit.

In order to determine the dependence of the ice-liquid equilibrium temperature on concentration, it is assumed that a_w is independent of temperature. Water activity for aqueous citric acid solutions are plotted for temperatures ranging from 250.7 to 319.33 K in Fig. A1. There is not a strong dependence of a_w in this temperature range; if there were the results would be scattered around the line of best fit. A significant dependence of a_w at lower temperatures can not be ruled out; however, similar assumptions have been made and justified in the past for other aqueous systems (Koop et al., 2000). The ice-liquid equilibrium curve in Fig. 5 was therefore calculated using Eq. (A1) and Eqs. (1) and (2) from Koop et al. (2000).

Appendix B

Determination of the lines of constant x_{H_2O} in Fig. 5

The determination of lines of constant mean diffusion distance was described in detail previsously (Murray, 2008), but is summarised here. The steep dependence of viscosity above T_g in aqueous solutions can be described by the WLF (Williams-Landel-Ferry) equation (Debenedetti, 1996):

$$\log \eta_T = \log \eta_{Tg} - \left(\frac{17.44(T - T_g)}{51.6 + (T - T_g)} \right) \quad \text{(B1)}$$

The dependence of molecular diffusion (D) of species i with viscosity can be approximated by the Stokes-Einstein equation (Debenedetti, 1996):

$$D_i = \frac{kT}{6\pi \eta_T r_i} \quad \text{(B2)}$$

where k is the Boltzmann constant and r_i is the hydrodynamic radius of i. Finally, the root mean square distance molecules of species i diffuse in a time (t) can be described by

$$x_i = (6 D_i t)^{0.5} \quad \text{(B3)}$$

In Fig. 5, lines of constant mean diffusion distance for water molecules (x_{H_2O}=0.001, 0.01, 0.1 and 1 μm) are plotted for a time period of 60 s. In this calculation r_{H_2O} was assumed to be identical in citric acid solutions to supercooled water at 244 K (r_{H_2O}=0.94Å, given that $D_{H_2O}=1.9\times10^{-10}$ m^2 s^{-1} and η=10 cP (Debenedetti, 1996)) and η_{Tg} was taken as 10^{14} cP.

Acknowledgements. The author thanks D. Wright for help running the X-ray diffractometer and A. K. Bertram, T. Koop, S. Dobbie, O. Möhler and T. Leisner for helpful discussions and B. K. James for proofreading this manuscript. The author acknowledges the Natural Environment Research Council (NE/D009308/1) and the School of Chemistry for funding.

Edited by: D. Cziczo

References

Abbatt, J. P. D.: Interactions of atmospheric trace gases with ice surfaces: Adsorption and reaction, Chem. Rev., 103, 4783–4800, 2003.

Angell, C. A.: Liquid fragility and the glass transition in water and aqueous solutions, Chem. Rev., 102, 2627–2650, 2002.

Apelblat, A., Dov, M., Wisniak, J., and Zabicky, J.: Osmotic and activity coefficients of ho2cch2c(oh)(co2h)ch2co2h (citric acid) in concentrated aqueous solutions at temperatures from 298.15 K to 318.15 K, J. Chem. Thermodynamics., 27, 347–353, 1995.

Apelblat, A.: Cryoscopic studies in the citric acid-water system, J. Mol. Liq., 103–104, 201–210, 2003.

Bogdan, A., Molina, M. J., Sassen, K., and Kulmala, M.: Formation of low-temperature cirrus from H_2SO_4/H_2O aerosol droplets, J. Phys. Chem. A, 110, 12 541–12 542, 2006.

Cziczo, D. J., DeMott, P. J., Brooks, S. D., Prenni, A. J., Thomson, D. S., Baumgardner, D., Wilson, J. C., Kreidenweis, S. M., and Murphy, D. M.: Observations of organic species and atmospheric ice formation, Geophys. Res. Lett., 31, L12116, doi:10.1029/2004GL019822, 2004a.

Cziczo, D. J., Murphy, D. M., Hudson, P. K., and Thomson, D. S.: Single particle measurements of the chemical composition of cirrus ice residue during crystal-face, J. Geophys. Res.-Atmos., 109, D04201, doi:10.1029/2003JD004032, 2004b.

Debenedetti, P. G.: Metastable liquids concepts and principles, Princeton University Press, New Jersey, 1996.

DeMott, P. J.: Laboratory studies of cirrus cloud processes, in: Cirrus, edited by: Lynch, D. K., Sassen, K., Starr, D. C., and Stephens, G., Oxford University Press, Oxford, 102–135, 2002.

DeMott, P. J., Cziczo, D. J., Prenni, A. J., Murphy, D. M., Kreidenweis, S. M., Thomson, D. S., Borys, R., and Rogers, D. C.: Measurements of the concentration and composition of nuclei for cirrus formation, Proc. Natl. Acad. Sci. USA, 100, 14 655–14 660, 2003.

Denman, K. L., Brasseur, G., Chidthaisong, A., Ciais, P., Cox, P. M., Dickinson, R. E., Hauglustaine, D., Heinze, C., Holland, E., Jacob, D., Lohmann, U., Ramachandran, S., da Silva Dias, P. L., Wofsy, S. C., and Zhang, X.: Couplings between changes in the climate system and biogeochemistry, in: Climate change 2007: The physical science basis. Contribution of working group i to the fourth assessment report of the intergovernmental panel on climate change, edited by: Solomon, S. D., Qin, M., Manning, Z., Chen, M., Marquis, K. B., Averyt, M. T., and Miller, H. L., Cambridge University Press, Cambridge, 2007.

Falkovich, A. H., Graber, E. R., Schkolnik, G., Rudich, Y., Maenhaut, W., and Artaxo, P.: Low molecular weight organic acids in aerosol particles from rondonia, brazil, during the biomass-burning, transition and wet periods, Atm. Chem. Phys., 5, 781–797, 2005.

Gao, R. S., Popp, P. J., Fahey, D. W., Marcy, T. P., Herman, R. L., Weinstock, E. M., Baumgardner, D. G., Garrett, T. J., Rosenlof, K. H., Thompson, T. L., Bui, P. T., Ridley, B. A., Wofsy, S. C., Toon, O. B., Tolbert, M. A., Karcher, B., Peter, T., Hudson, P. K., Weinheimer, A. J., and Heymsfield, A. J.: Evidence that nitric acid increases relative humidity in low-temperature cirrus clouds, Science, 303, 516–520, 2004.

Gettelman, A. and Forster, P. M. D.: A climatology of the tropical tropopause layer, J. Meteor. Soc. Japan, 80, 911–924, 2002.

Graber, E. R. and Rudich, Y.: Atmospheric hulis: How humic-like are they? A comprehensive and critical review, Atm. Chem. Phys., 6, 729–753, 2006.

Jensen, E. and Pfister, L.: Implications of persistent ice supersaturation in cold cirrus for stratospheric water vapor, Geophys. Res. Lett., 32, D03208, doi:03210.01029/02004GL021125, 2005.

Jensen, E. J., Smith, J. B., Pfister, L., Pittman, J. V., Weinstock, E. M., Sayres, D. S., Herman, R. L., Troy, R. F., Rosenlof, K., Thompson, T. L., Fridlind, A. M., Hudson, P. K., Cziczo, D. J., Heymsfield, A. J., Schmitt, C., and Wilson, J. C.: Ice supersaturations exceeding 100% at the cold tropical tropopause: Implications for cirrus formation and dehydration, Atm. Chem. Phys., 5, 851–862, 2005.

Kärcher, B. and Koop, T.: The role of organic aerosols in homogeneous ice formation, Atm. Chem. Phys., 5, 703–714, 2005.

Koop, T., Ng, H. P., Molina, L. T., and Molina, M. J.: A new optical technique to study aerosol phase transitions: The nucleation of ice from h2so4 aerosols, J. Phys. Chem. A., 102, 8924–8931, 1998.

Koop, T., Bertram, A. K., Molina, L. T., and Molina, M. J.: Phase transitions in aqueous nh4hso4 solutions, J. Phys. Chem. A., 103, 9042–9048, 1999.

Koop, T., Luo, B. P., Tsias, A., and Peter, T.: Water activity as the determinant for homogeneous ice nucleation in aqueous solutions, Nature, 406, 611–614, 2000.

Koop, T.: Homogeneous ice nucleation in water and aqueous solutions, Z. Phys. Chem., 218, 1231–1258, 2004.

Levien, B. J.: A physicochemical study of aqueous citric acid solutions, J. Phys. Chem., 59, 640–644, 1955.

Liou, K.-T.: Influence of cirrus clouds on weather and climate processes: A global persepective, Mon. Weath. Rev., 114, 1167–1199, 1986.

Maffia, M. C. and Meirelles, J. A.: Water activity and ph in aqueous polycarboxylic acid systems, J. Chem. Eng. Data, 46, 582–587, 2001.

Maltini, E., Anese, M., and Shtylla, I.: State diagrams of some organic acid-water systems of interest in food, Cryo-Letters, 18, 263–268, 1997.

McFiggans, G., Alfarra, M. R., Allan, J., Bower, K., Coe, H., Cubison, M., Topping, D., Williams, P., Decesari, S., Facchini, C., and Fuzzi, S.: Simplification of the representation of the organic component of atmospheric particulates, Faraday Discuss., 130, 341–362, 2005.

Möhler, O., Linke, C., Saathoff, H., Schnaiter, M., Wagner, R., Mangold, A., Kramer, M., and Schurath, U.: Ice nucleation on flame soot aerosol of different organic carbon content, Meteorologische Zeitschrift, 14, 477–484, 2005.

Murphy, D. M., Thomson, D. S., and Mahoney, T. M. J.: In situ measurements of organics, meteoritic material, mercury, and other elements in aerosols at 5 to 19 km, Science, 282, 1664–1669, 1998.

Murphy, D. M. and Koop, T.: Review of the vapour pressures of ice and supercooled water for atmospheric applications, Q. J. Roy. Meteor. Soc., 131, 1539–1565, 2005.

Murphy, D. M., Cziczo, D. J., Froyd, K. D., Hudson, P. K., Matthew, B. M., Middlebrook, A. M., Peltier, R. E., Sullivan, A., Thomson, D. S., and Weber, R. J.: Single-particle mass spectrometry of tropospheric aerosol particles, J. Geophys. Res.-Atmos., 111, D23S32, doi:10.1029/2006JD007340, 2006.

Murray, B. J., Knopf, D. A., and Bertram, A. K.: The formation of cubic ice under conditions relevant to earth's atmosphere, Nature, 434, 202–205, 2005.

Murray, B. J. and Bertram, A. K.: Formation and stability of cubic ice in water droplets, Phys. Chem. Chem. Phys., 8, 186–192, 2006.

Murray, B. J. and Bertram, A. K.: Laboratory studies of the formation of cubic ice in aqueous droplets, in: Physics and chemistry of ice, edited by: Kuhs, W. F., The Royal Society of Chemistry, Cambridge, 417–426, 2007a.

Murray, B. J. and Bertram, A. K.: Strong dependence of cubic ice formation on droplet ammonium to sulfate ratio, Geophys. Res. Lett., 34, L16810, doi:10.1029/2007GL030471, 2007b.

Murray, B. J.: Enhanced formation of cubic ice in aqueous organic acid droplets, Env. Res. Lett., 3, 025008, doi:025010.021088/021748-029326/025003/025002/025008, 2008.

Murray, B. J. and Bertram, A. K.: Inhibition of solute crystallisation in aqueous H^+–NH_4^+–SO_4^{2-}–H_2O droplets Phys. Chem. Chem. Phys., 10, 3287–3301, doi:3210.1039/B802216J, 2008.

Peng, C., Chan, M. N., and Chan, C. K.: The hygroscopic properties of dicarboxylic and multifunctional acids: Measurements and unifac predictions, Environ. Sci. Technol., 35, 4495–4501, 2001.

Peter, T., Marcolli, C., Spichtinger, P., Corti, T., Baker, M. B., and Koop, T.: When dry air is too humid, Science, 314, 1399–1402, 2006.

Prenni, A. J., DeMott, P. J., Kreidenweis, S. M., Sherman, D. E., Russell, L. M., and Ming, Y.: The effects of low molecular weight dicarboxylic acids on cloud formation, J. Phys. Chem. A, 105, 11 240–11 248, 2001.

Saxena, P. and Hildemann, L. M.: Water-soluble organics in atmospheric particles: A critical review of the literature and applications of thermodynamics to identify candidate compounds, J. Atm. Chem., 24, 57–109, 1996.

Taylor, N. W.: Solubility of organic substances and of weak electrolytes in water, in: International critical tables of numerical data, physics, chemistry and technology, edited by: Washburn, McGraw-Hill, New York, 263, 1926.

Wise, M. E., Garland, R. M., and Tolbert, M. A.: Ice nucleation in internally mixed ammonium sulfate/dicarboxylic acid particles, J. Geophys. Res. Atm., 109, D19203, doi:10.1029/2003JD004313, 2004.

Zhou, X. L., Geller, M. A., and Zhang, M. H.: Temperature fields in the tropical tropopause transition layer, J. Climate, 17, 2901–2908, 2004.

Zobrist, B., Weers, U., and Koop, T.: Ice nucleation in aqueous solutions of poly[ethylene glycol] with different molar mass, J. Chem. Phys., 118, 10254-10261, 2003.

Zobrist, B., Marcolli, C., Koop, T., Luo, B. P., Murphy, D. M., Lohmann, U., Zardini, A. A., Krieger, U. K., Corti, T., Cziczo, D. J., Fueglistaler, S., Hudson, P. K., Thomson, D. S., and Peter, T.: Oxalic acid as a heterogeneous ice nucleus in the upper troposphere and its indirect aerosol effect, Atmos. Chem. Phys, 6, 3115–3129, 2006.

Zobrist, B., Marcolli, C., Pedernera, D. A., and Koop, T.: Do atmospheric aerosols form glasses?, Atmos. Chem. Phys., 8, 5221–5244, 2008, http://www.atmos-chem-phys.net/8/5221/2008/.